



# City-wide model-based analysis of heat recovery from wastewater using an uncertainty-based approach



R. Saagi<sup>a,\*</sup>, M. Arnell<sup>a,b</sup>, C. Wärff<sup>a,b</sup>, M. Ahlström<sup>b</sup>, U. Jeppsson<sup>a</sup>

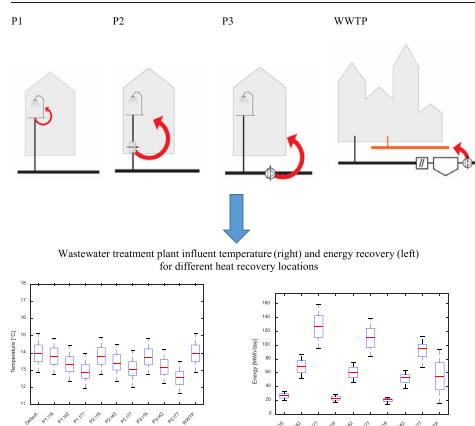
<sup>a</sup> Division of Industrial Electrical Engineering and Automation (IEA), Department of Biomedical Engineering, Lund University, PO Box 118, SE-22100 Lund, Sweden

<sup>b</sup> RISE Research Institutes of Sweden, Gjuterigatan 1D, SE-58273 Linköping, Sweden

## HIGHLIGHTS

- Heat recovery from wastewater is evaluated using an uncertainty-based approach.
- Heat recovery at showers (77%) gives highest mean energy recovery.
- Maximum mean temperature drop (precinct level with 77%) is 1.5 °C.
- Impact on WWTP performance is negligible due to the special configuration.

## GRAPHICAL ABSTRACT



## ARTICLE INFO

### Article history:

Received 3 December 2021

Received in revised form 13 January 2022

Accepted 15 January 2022

Available online 22 January 2022

Editor: Huu Hao Ngo

### Keywords:

Heat recovery

Wastewater

City-wide modelling

Uncertainty analysis

## ABSTRACT

Around 90% of the energy requirement for urban water systems management is for heating domestic tap water. In addition, the energy content of wastewater is mainly in the form of heat (85%). Hence, there is an obvious interest in recovering a large portion of this heat. However, city-wide scenario analyses that evaluate heat recovery at various locations while considering impacts on wastewater treatment plant (WWTP) performance are currently very limited. This study presents a comprehensive model-based city-wide evaluation considering four different heat recovery locations (appliance, household, precinct and WWTP effluent) for a Swedish city with varying degrees of implementation using an uncertainty-based approach. Results show that heat recovery at the appliance level, with heat exchangers installed at 77% of the showers at domestic households, leads to a mean energy recovery of 127 MWh/day with a 0.25 °C reduction in mean WWTP inlet temperature compared to the default case without heat recovery. The highest mean temperature reduction compared to the default case is 1.5 °C when heat is recovered at the precinct level for 77% of the domestic wastewater flow rate. Finally, the impact on WWTP nitrification capacity is negligible in this case due to its large existing capacity and design.

\* Corresponding author at: Div. of Industrial Electrical Engineering and Automation (IEA), Dept. of Biomedical Engineering (BME), Lund University, IEA, PO Box 118, SE-22100 Lund, Sweden.

E-mail addresses: [ramesh.saagi@iea.lth.se](mailto:ramesh.saagi@iea.lth.se)

URL: <http://www.iea.lth.se/> (R. Saagi), [magnus.arnell@ri.se](mailto:magnus.arnell@ri.se) (M. Arnell), [christoffer.warff@ri.se](mailto:christoffer.warff@ri.se) (C. Wärff), [marcus.ahlstrom@ri.se](mailto:marcus.ahlstrom@ri.se) (M. Ahlström), [ulf.jeppsson@iea.lth.se](mailto:ulf.jeppsson@iea.lth.se) (U. Jeppsson).

## 1. Introduction

Two of the key targets for the year 2030 set by the European Union climate and energy framework are: at least 32% share for renewable energy; and at least 32.5% improvement in energy efficiency (European Union, 2019). This includes heat recovered from wastewater (Directive (EU) 2018/2001, 2018). In the current situation, where energy is usually not recovered from wastewater, a significant portion (90%) of the energy required for urban water systems management is used for heating tap water (Olsson, 2012). Furthermore, 85% of the energy content in wastewater is in the form of heat while the rest is organic material and nutrients (Larsen, 2015). The Swedish Energy Agency (2009) has estimated that energy requirement for domestic hot water is 1150 kWh/cap/yr. Several studies demonstrate that a significant part of the energy used to meet this heating demand can be recovered using wastewater heat recovery. Heat recovery ratios ranging from 17% to 42% are observed by a Swedish study that analysed different heat recovery installations (Wallin, 2021). Several other international examples of such installations are also available in literature (Nagpal et al., 2021; Petersen, 2018; Vavříčka et al., 2022).

In general, four major locations for heat recovery can be broadly defined (Arnell et al., 2017):

1. Appliances level (showers, dishwashers, etc.)
2. Household level
3. Precinct level (sewer network or a pumping station)
4. System level (WWTP effluent)

Several heat recovery solutions are now available in the market for all these locations. Heat exchangers are commonly used for small and irregular flow conditions typically at an appliance or household level. For heat recovery from precincts/sewer systems and WWTP effluents, heat pumps are used for a more efficient energy recovery. Several large WWTPs in Sweden and elsewhere already have heat recovery from the WWTP effluent (Chae and Ren, 2016; Petersen, 2018) or are actively evaluating such possibilities (Spriet et al., 2020).

With growing interest in heat recovery installations, it is important to evaluate the energy recovery potential at a system-wide scale to identify the most effective heat recovery locations by taking into consideration the potential effects of heat recovery on downstream processes, like WWTPs. A particular concern is the negative impact on WWTP operation, mainly nitrification, due to the decreased wastewater temperature caused by upstream heat recovery (Wanner et al., 2005). Model-based system-wide evaluation can be a valuable tool for decision-making taking into consideration not only energy recovery potential but also downstream impacts on WWTPs and other aspects.

Such an evaluation will require different sub-models for: 1. Wastewater generation from households (flow rate and temperature); 2. Sewer heat transfer; 3. WWTP; and 4. Heat recovery equipment. Models for each of these components exist at various levels of complexity, although limited full-scale applications are currently available. Wastewater generation is calculated using either a standard dry weather profile together with information on the population equivalents and the average per capita daily wastewater generation (Abdel-Aal et al., 2018) or a stochastic model based on usage statistics for each of the different household wastewater generation sources (Sitzenfrei et al., 2017; Wärrff et al., 2020). Sewer heat transfer models are initially developed as detailed two-dimensional models (Dürrenmatt and Wanner, 2014; Elías-Maxil et al., 2017). One-dimensional models that consider the major heat transfer phenomena are also present. In general, one-dimensional sewer heat transfer models include a detailed hydraulic model that is integrated with a heat transfer model either in the same platform (Figuroa et al., 2021; Saagi et al., 2021) or by integrating information from different software (Abdel-Aal et al., 2014). Conceptual flow rate and heat transfer models that further simplify the model complexity and reduce data requirements for model development are also described (Saagi et al., 2021). WWTP models that include energy impacts describing all the interactions at a plant-wide level are developed (Fernández-Arévalo et al., 2014, 2017). Other studies consider only the major heat transfer

processes and integrate them into the existing activated sludge models (Arnell et al., 2021; Lippi et al., 2009). For heat recovery equipment models, detailed models including system configuration (Hadengue et al., 2022) as well as steady-state models for heat exchangers and heat pumps are used (Arnell and Saagi, 2020). In other cases, energy recover calculations (potential energy recovery and reduction in downstream temperature) are directly calculated without any separate equipment model (Abdel-Aal et al., 2018).

Limited city-wide case studies are currently available with varying levels of complexity (Abdel-Aal et al., 2018; Golzar and Silveira, 2021; Hadengue et al., 2021). The current studies generally predict the WWTP influent temperature but do not directly integrate it with a WWTP model. The wastewater generation aspect is usually simplified and many studies do not have the information to evaluate appliance level heat recovery. The sewer models used are generally detailed hydraulic models either using existing hydraulic modelling software or developed using the same principles. Conceptual sewer models can be valuable to overcome the complexity in modelling the lateral connections to the main sewer systems while still considering their impact on heat transfer in the sewer system.

In this study, a comprehensive system-wide analysis is carried out for the Swedish city of Linköping. Several potential heat recovery alternatives (appliance, household, precinct and WWTP level) with varying degrees of implementation are evaluated in terms of energy recovery potential as well as their impact on WWTP inlet temperature and eventually nitrification performance at the WWTP. Additionally, uncertainty analysis is incorporated to support robust decision-making. The study integrates several novel aspects for a city-wide heat recovery analysis, namely: i. Dynamic flow rate and temperature information for appliance and household level heat recovery; ii. Combination of conceptual and mechanistic sewer heat transfer models to overcome limited data availability and model complexity; iii. Heat recovery equipment models for heat exchangers and heat pumps; and finally, iv. Integration of upstream models with a calibrated and validated WWTP model. The sub-models for the different components are all developed in the same simulation platform (Matlab) and interconnected for a holistic analysis. All the source code used for the underlying models is open-source and the models are distributed freely at Github (<https://github.com/wwtmodels/Wastewater-Heat-Recovery-Models>).

## 2. Methods

### 2.1. Model description

Four major sub-models are integrated, namely: 1. Wastewater generation model (Wärrff et al., 2020); 2. Sewer heat transfer model (Saagi et al., 2021); 3. WWTP model (Arnell et al., 2021); and 4. Heat recovery equipment models (Arnell and Saagi, 2020).

#### 2.1.1. Wastewater generation model

The stochastic wastewater generation model (Wärrff et al., 2020) is used to generate pollutant loads, flow rate and temperature input data for households. The model is based on the daily usage patterns for the different end-use types (shower, bath, WC, dishwasher, washing machine and taps). The information is gathered from The Swedish Energy Agency (2009) and Sitzenfrei et al. (2017). This includes, for each end-use type:

- Volume of water used per usage;
- Frequency of usage per day;
- The mean and standard deviation for the temperature of generated wastewater;
- The mean and standard deviation for the flow rate of generated wastewater;
- The mean and standard deviation for the duration of appliance usage;
- The mean and standard deviation for the time of usage (each day is divided into 4 periods) for weekdays and weekends.

The daily usage patterns are used to generate probability distribution functions for the different end-use types. Additionally, it needs information

on the number of connected inhabitants, no. of days for which household wastewater data should be generated, incoming cold-water temperature and the outgoing domestic hot water temperature from the heating system. This information is case-specific and can be easily modified by users.

At each sample time (sample frequency is user-defined) and for each PE, the above probability distribution functions are sampled and combined to generate the flow rate and temperature value for each end-use type. Also, pollutant loads (particulate chemical oxygen demand (COD), soluble COD, ammonical nitrogen, total Kjeldahl nitrogen, total phosphorus) are collated from various sources for each end-use type as loads (g/usage) which is used to calculate pollutant concentrations at each time interval. All the information generated is summarized to generate the total pollutant concentration, flow rate and temperature values for wastewater from each sub-catchment. Finally, heat loss as the wastewater flows through the sewer pipes in the household to the external sewer system is calculated using an empirical equation (Sitzenfrei et al., 2017).

### 2.1.2. Sewer heat transfer model

The sewer model (Saagi et al., 2021) describes wastewater temperature variations in sewer systems using one-dimensional energy balance equations considering key processes for heat transfer in sewer systems (conduction, convection and biochemical heat generation) (Abdel-Aal et al., 2014, 2018; Saagi et al., 2021). Two different approaches are available:

1. Mechanistic model – One-dimensional heat transfer processes for heat exchange between: in-sewer air and wastewater; wastewater and sewer concrete pipe; sewer pipe and surrounding soil are considered in the overall energy balance. Two state variables are used to describe temperature variation in wastewater as well as the sewer pipe material. The flow rate is modelled using a kinematic wave approximation of the standard St. Venant's equation.
2. Conceptual model – All the heat transfer processes are lumped into a single heat transfer equation where the heat transfer coefficient is a function of the flow rate (Monod function). The driving force is the temperature difference between wastewater and in-sewer air temperature (for gravity sewers)/soil temperature (for pumped sewers). Flow rate is modelled using a series of reservoirs approach.

Both models are available for gravity and pumped sewer networks. While the mechanistic model needs detailed information about the sewer pipe characteristics, the conceptual model needs very limited flow rate information for model calibration.

In order to describe the soil temperature for the entire year, a simple sine-wave based model is developed where soil temperature variation across the entire year is simulated and used as input to the sewer heat transfer model. The mean annual temperature, amplitude and phase-change of the sine-wave are used as model parameters. This enables the use of the model for long-term studies without having to adjust the soil temperature on a monthly/seasonal basis.

### 2.1.3. Wastewater treatment plant model

The WWTP model (Arnell et al., 2021) integrates temperature flux equations with the unit operation models in the plant-wide Benchmark Simulation Model no. 2 (BSM2) (Gernaey et al., 2014) used in this study. Temperature variation is included in all the bioreactor models using a net energy flux that considers several processes: solar radiation; atmospheric radiation; conduction and convection; evaporation; aeration, sensible and latent heat losses and biological processes (Arnell et al., 2021; Lippi et al., 2009; Makinia et al., 2005). The models include the capability to dynamically adapt to seasonal variations making them suitable for long-term simulations. Apart from the wastewater process data for model calibration, the temperature model also needs information about solar radiation, wind speed, air temperature, humidity, barometric pressure, etc. A modified version of activated sludge model no. 1 (ASM1) (Henze et al., 2000) is used to describe the activated sludge units. The process models for all the other bioprocesses are based on the BSM2 framework (Gernaey et al., 2014).

### 2.1.4. Heat recovery equipment models

Two different heat recovery equipment models are developed.

#### a. Heat exchangers

Counter-current flow heat exchanger units are modelled using standard energy balance equations (Geankoplis, 1993).

$$q = \varepsilon \cdot C_{\min} (T_{h,\text{in}} - T_{c,\text{in}}) \quad (1)$$

$$C_{\min} = \min_{i=c,h} (\dot{m} \cdot c_p)_i \quad (2)$$

$$T_{h,\text{out}} = T_{h,\text{in}} - \frac{q}{(\dot{m} \cdot c_p)_h} \quad (3)$$

$$T_{c,\text{out}} = T_{c,\text{in}} + \frac{q}{(\dot{m} \cdot c_p)_c} \quad (4)$$

where,  $q$  [kW] is the actual heat transfer,  $\varepsilon$  [-] is the effectiveness of the heat exchanger,  $C_{\min}$  [kW/K] is the minimum heat capacity,  $T_{i,j}$  [°C] is the temperature – index  $i$  indicates cold (c) or hot media (h), index  $j$  denotes in- or outgoing temperature,  $\dot{m}_i$  [kg/s] is the mass transfer rate and  $c_p$  [kJ/kg·K] is the heat capacity – index  $i$  denote cold or hot media. The model outputs from the heat exchanger are  $T_{c,\text{out}}$  (output temperature of the heated water) and  $T_{h,\text{out}}$  (output temperature of wastewater).

#### b. Heat pumps

The layout of a heat pump installation that is typically used in wastewater heat recovery applications is given in Fig. 1. It consists of a heat exchanger and a heat pump. Heat from wastewater is transferred to an internal coolant (cold media) through the heat exchanger. This prevents wastewater from getting in direct contact with the evaporator. The energy from the cold media is then transferred to warm media (used for district heating) through a heat pump in a series of steps: 1. Additional energy is used to raise the temperature of the cold media using a compressor; 2. This heat is transferred to the warm media through a condenser and the cold media temperature reduces further after passing through the throttle valve; 3. The cold media is then heated again using the energy from wastewater. The heat capacity and density values for the different media are given in Table 1.

The heat pump system is modelled using standard equations (Geankoplis, 1993).

$$E_{\text{cond}} = -P \cdot \text{COP} \quad (5)$$

$$T_{c,\text{out}} = T_{c,\text{in}} - \frac{|E_{\text{cond}}| - P}{(\dot{m} \cdot c_p)_c} \quad (6)$$

$$T_{h,\text{out}} = T_{h,\text{in}} - \frac{E_{\text{cond}}}{(\dot{m} \cdot c_p)_h} \quad (7)$$

where,  $E_{\text{cond}}$  is the energy transferred in the condenser [kW]. The key design parameters are power input ( $P$ ) [kW] and coefficient of performance (COP) [-]. A standard design for heat pump installation is scaled for the different locations based on the incoming flow rate (Table 1). Additionally, a feedback controller (PI control) is designed to ensure that the outgoing warm media always attains the desired temperature. The incoming warm media has a fixed temperature (30 °C) and its flow rate is manipulated (depending on the available heat content in the wastewater) to attain a fixed output warm media temperature (60 °C). The flow rate of the internal cold media is fixed. The power input is also limited to a maximum value so that the cold media does not reach temperatures lower than 0 °C. While several possibilities exist (high degree of freedom), this approach is followed in all the model simulations to ensure that the simulation results are comparable.

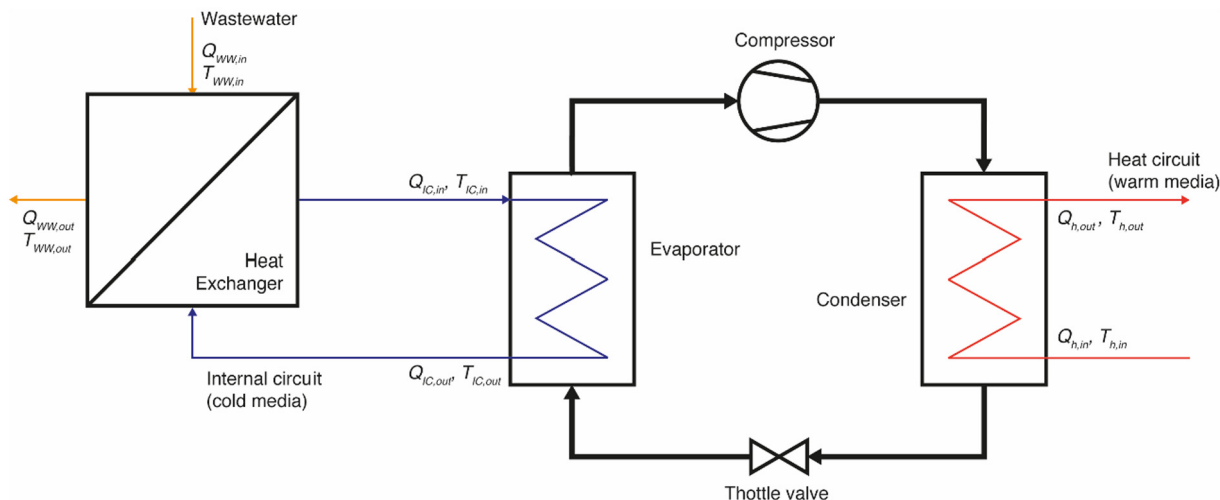


Fig. 1. Principal illustration of heat pump for wastewater application. (Adapted from Arnell and Saagi (2020)).

2.2. Linköping case-study details

The Linköping urban catchment has a total of 180,000 population equivalents (PE) that are distributed across 32 sub-catchments. Two additional sub-catchments are used to simulate industrial wastewater generation. The division of the urban catchments into different sub-catchments and identification of the PE and area for each sub-catchment are carried out by the utility Tekniska Verken in Linköping AB, which manages the sewer system and the wastewater treatment plant in Linköping. Major manhole locations in the sewer network are used as nodes for the sub-catchments (Fig. 2). Average wastewater flow rate at WWTP inlet is 43,000 m<sup>3</sup>/d, which consists of wastewater from domestic sources, industries (20%) and infiltration to sewers during dry weather conditions (10%). Majority of the sewer network consists of gravity sewers with a few pumped sewer pipes.

Primary treatment consists of grit removal, pre-aeration and chemically enhanced primary clarification (Fig. 3). The biological treatment consists of three parallel activated sludge units with intermittent aeration followed by secondary clarifiers. Tertiary treatment with ozonation for micropollutant removal is followed by moving bed biological reactors (MBBR) in series for post nitrification and denitrification (N-DN). Finally, a post-precipitation and clarification unit are used after which the effluent is discharged into the receiving waters. The mixed sludge from primary clarifiers reaches the thickener and is then sent to three interconnected digesters for anaerobic digestion. The sludge from digesters is dewatered and the reject water subjected to further nitrogen removal through side-stream treatment. The reject water is sent back to the influent while the remaining sludge from the dewatering unit is sent for disposal or reuse. Models for the specific sub-processes are also included in Arnell et al. (2021).

2.3. Integrating the sub-models and model calibration

A calibrated and validated wastewater generation model (Wärff et al., 2020) is used for generating wastewater flow rate and temperature values

Table 1  
Standard design values used for scaling the heat pump model for different locations (Arnell and Saagi, 2020).

	Q [m <sup>3</sup> /d]	Heat capacity (kJ/kg·K)	Density (kg/m <sup>3</sup> )
Wastewater	3283	4.181	998.2
Cold media (internal circuit)	2073	3.87	1036
Warm media (domestic hot water)	4406	4.194	999.7

from the 32 domestic sub-catchments based on data from Linköping and other sources. The wastewater for each domestic sub-catchment is generated based on the PE data for the sub-catchment as well as daily average drinking water temperature data for the entire year. The outputs from the wastewater generation model are flow rate and temperature at 15-minute time intervals for: wastewater from showers only; wastewater from rest of the household; incoming cold water to the heat exchangers at showers; and incoming cold water to the heat exchanger for the entire household. The separation of the total household wastewater into two components, showers and rest of the households, allows for the evaluation of two heat recovery possibilities – appliance level (at showers) and household level. The outputs from the wastewater generation model are saved and used as inputs to the sewer network model. Two industrial sub-catchments are assumed with constant wastewater flow rate and temperature due to the lack of detailed dynamic data. A temperature of 22 °C is used for the industrial wastewater based on discussions with the utility managers at Tekniska Verken i Linköping AB.

The sewer network is modelled using the conceptual and mechanistic sewer temperature models described by Saagi et al. (2021) that simulates both the flow rate and temperature dynamics in the sewer system. The sewer pipes within the sub-catchment are represented as a series of conceptual reservoir models for each sub-catchment. A constant infiltration flow rate (10% of the domestic wastewater flow rate) is added for each sub-catchment. The soil temperature and infiltration water temperature are assumed to be similar as measurements are not available (Figuroa et al., 2021). The model parameters for the conceptual and detailed models are calibrated based on wastewater temperature and flow rate data at the WWTP inlet. The conceptual flow rate model is calibrated first followed by the calibration of the conceptual and detailed sewer model parameters simultaneously. The model parameters are manually calibrated based on the comparison between measured and modelled wastewater temperature at the WWTP inlet. For the soil temperature model, since no data is available for model calibration, literature values from Forsberg et al. (2012) and Kjellander (2015) as well as model results from a detailed soil temperature model (HYDROS) (Šimůnek et al., 2016) using air temperature as input data are used as the basis. Calibration for the sewer model is based on data from 15 Jan.–04 Feb. 2020 (period 1) while validation is from 15 April–04 May 2020 (period 2).

The calibrated and validated WWTP model from Arnell et al. (2021) is used in this study. The IWA good modelling practices guideline is followed for model development, calibration and validation (Rieger et al., 2012). The flow rate and temperature values from the upstream sewer model and pollutant load data from the year 2019 are used as model inputs. A local weather station is installed, measuring all necessary input variables

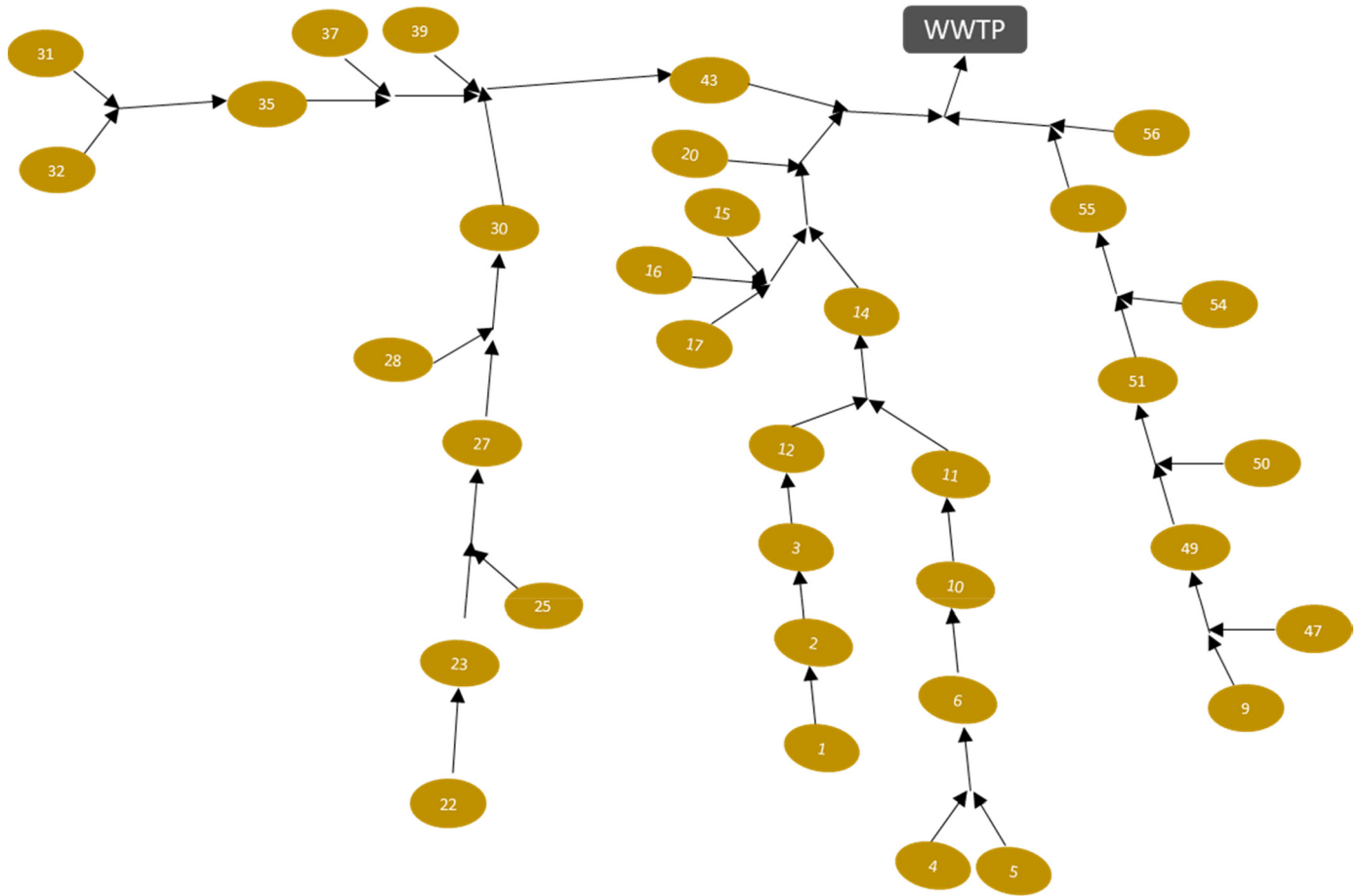


Fig. 2. Overview of the Linköping urban catchment and the different sub-catchments used for modelling heat recovery from wastewater.

for the heat flux model. Gaps in data, for example due to short-term failure in local measurements, are filled with corresponding data from nearby sites recorded by the Swedish Meteorological and Hydrological Institute (SMHI).

The efficiency factors for the shower and household heat exchangers are assumed as 0.49 and 0.52 based on literature values (Arnell and Saagi, 2020) and also assuming that heat recovery directly at the showers is more efficient than that at the household level. Heat exchangers at shower

and household level are modelled for 32 catchments. No heat exchangers/heat pumps are simulated at the industrial catchments as the study focuses on heat recovery scenarios mainly from domestic wastewater and no detailed wastewater generation data/model is available for the industrial wastewater.

The heat pump design mentioned in Table 1 is scaled for the different sub-catchments based on the wastewater flow from the sub-catchment.

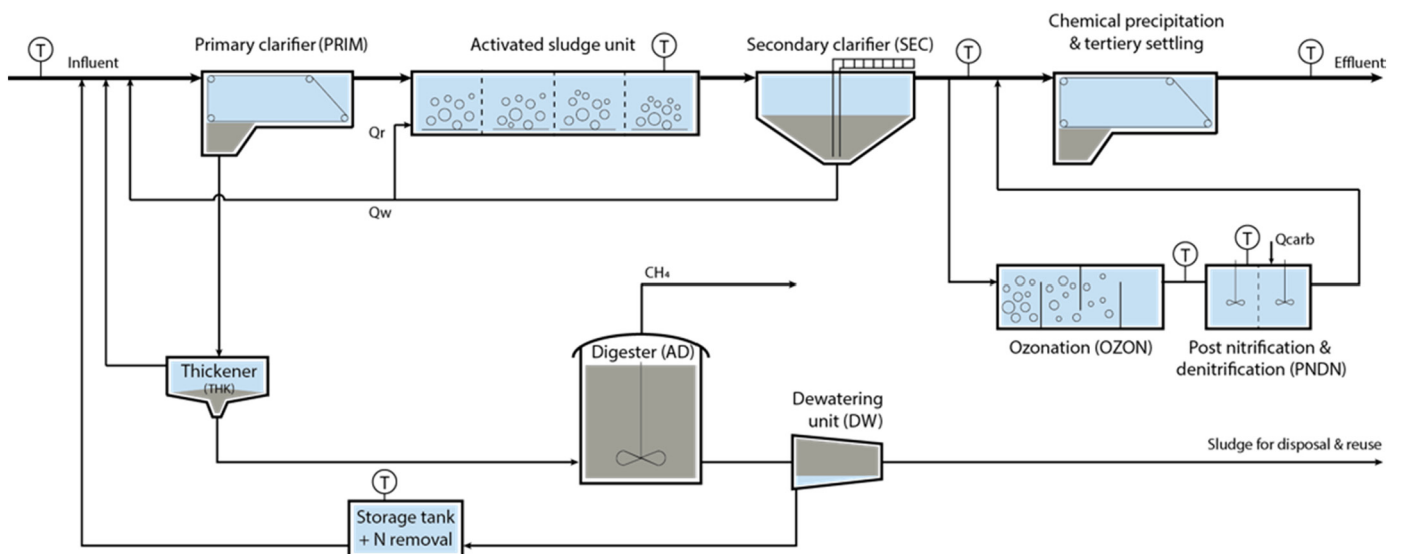


Fig. 3. Plant layout for the Linköping WWTP consisting of both the water line and the sludge line.

Similar scaling is also done for the heat pump at the WWTP. The heat pumps at the sub-catchment level have a coefficient of performance (COP) of 5.9 while that at the WWTP has a COP of 3.0, owing to the much larger flow rate and the lower wastewater temperature that it receives. The COP values are based on [Arnell and Saagi \(2020\)](#) and [Tikhonova \(2018\)](#).

#### 2.4. Heat recovery scenarios

Four potential heat recovery locations are selected for the study ([Fig. 4](#)).

1. Appliance level (P1) – Heat recovery from shower wastewater is achieved using heat exchangers. Incoming cold water to showers is pre-heated using the recovered heat.
2. Household/apartment level (P2) – The total wastewater from the household/apartment is used for heat recovery using a heat exchanger. Recovered heat is used to preheat domestic hot water for the household.
3. Precinct level (P3) – Heat pumps are used for heat recovery from a major sewer pipe or pumping station that receives all the wastewater from a precinct or a sub-catchment. In this study, one heat pump is modelled for each of the 32 residential sub-catchments. The heat recovered from such a location is used for district heating.
4. System level (WWTP) – Heat from WWTP effluent is recovered using heat pumps. The recovered heat is generally used internally at the WWTP and/or for district heating.

For the first three locations (P1, P2, P3), different extents of implementation within the city are considered (16%, 42%, 77%) (e.g. for P1 – 16% implies that 16% of the domestic wastewater flow from showers in the city have heat exchangers installed for heat recovery). In order to simplify the model development, it is assumed that household and shower heat recovery will either be present or absent for all the households in a sub-catchment. Partial implementation of heat recovery at a sub-catchment level is not considered. At the WWTP, heat recovery is carried out for the entire effluent flow rate. In total, 11 scenarios are considered (default scenario without heat recovery, three scenarios each at P1, P2 and P3, and WWTP).

#### 2.5. Uncertainty analysis

In order to consider the uncertainty in various sources (model and design parameters), Monte-Carlo simulations with Latin hypercube sampling (LHS) ([Iman and Conover, 1982](#)) considering the correlation in the input parameters are designed ([Gatto and Drago, 2020](#); [Sin et al., 2009](#)).

Monte-Carlo methods are used to evaluate model uncertainty caused by variation in inputs and model parameters ([Saltelli et al., 2008](#)). Random samples from the input parameter space (with a predetermined uncertainty range) are fed to the model and variation in the model output is observed. Latin Hypercube Sampling ([Iman and Conover, 1982](#)) is an efficient method to sample the input parameter space ensuring that the variability

**Table 2**

List of parameters used for uncertainty analysis and their default values separated for each sub-model.

Variable name	Default value
Sewer heat transfer model - mechanistic	
Mean soil temperature ( $T_{\text{mean}}$ )	5 °C
Heat transfer coefficient from wastewater to in-sewer air ( $h_{\text{wa}}$ )	10 W/m <sup>2</sup> K
Thermal conductivity of concrete pipe ( $k_p$ )	5 W/m-K
Thermal conductivity of soil ( $k_s$ )	3 W/m-K
Pipe thickness ( $w_p$ )	0.15 m
Soil depth for heat transfer ( $d_s$ )	0.5 m
Reaction enthalpy for COD degradation ( $e_{\text{cod}}$ )	14 × 10 <sup>6</sup> J/kg
COD	
COD degradation rate in sewers ( $r_{\text{cod}}$ )	1 × 10 <sup>-6</sup> kg/m <sup>3</sup> s
Sewer heat transfer model - conceptual	
Overall heat transfer factor ( $h_{\text{sewer}}$ )	2500 W/K
$n_{\text{flow}}$	0.8
$K_{\text{res}}$	700 d <sup>-1</sup>
Heat recovery equipment model	
Efficiency of heat exchanger at household level ( $\epsilon$ )	0.49
Efficiency of heat exchanger at showers ( $\epsilon$ )	0.52
Coefficient of performance for heat pumps at precinct level (COP)	5.9
Coefficient of performance for heat pumps at WWTP (COP <sub>WWTP</sub> )	3
WWTP model	
Total volume of activated sludge reactors	13,340 m <sup>3</sup>
Primary clarifier volume	6200 m <sup>3</sup>
Secondary clarifier area	4956 m <sup>2</sup>

in the samples is representative of the input parameter variability. This is ensured by dividing the input parameter space into several sub spaces (so-called Latin Hypercubes). A random sample for each Latin Hypercube is chosen to ensure that the selected samples are coming from the entire input parameter space. A major advantage is that the input uncertainty can be represented with limited number of samples, leading to less simulations and computational efforts.

The list of parameters and their ranges are mentioned in the [Table 2](#). All the model parameters in the sewer heat transfer model are included as the model is not yet widely used and there is limited knowledge on the parameter uncertainty. The design parameters for the heat recovery models (heat exchangers and heat pumps) are included as uncertain parameters as the design in reality is case-specific and is difficult to generalize for the entire city. In terms of input data, since it has been difficult to gather soil temperature data or use a detailed soil temperature model, the annual mean soil temperature used in the sine-wave based soil model is added to the list of uncertain parameters. Finally, in order to also account for the uncertainty in the WWTP design values, volumes of the reactors are included. The area of the reactors has a strong influence on the heat losses in the WWTP. Hence, it is included in the uncertainty analysis. In total, 16 variables are considered for the uncertainty analysis. While the total volume

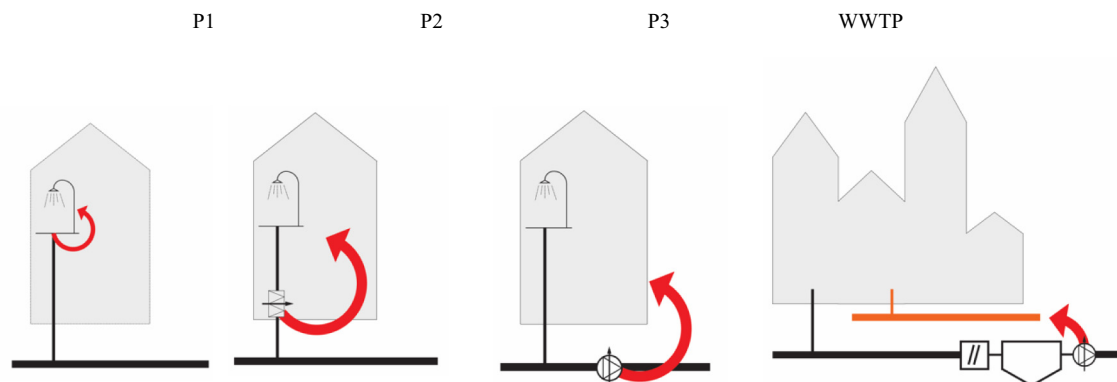


**Fig. 4.** Different positions for heat recovery from wastewater – showers (P1), households (P2), precincts (P3) and WWTP effluent (WWTP).

of activated sludge reactors and secondary clarifier area are represented in Table 2, the simulation model has several reactors. All these reactor volumes are considered separately for the uncertainty analysis. A high uncertainty range of 25% is used for all the variables. We consider this as a practically reasonable yet sufficiently high uncertainty range (Sin et al., 2009).

Latin hypercube sampling is used to sample the input parameter space efficiently. A modified LHS method that can handle correlations in the input variables is used (Iman and Conover, 1982). Uniform uncertainty range is used for all the variables. In total, 250 samples are generated for each simulation scenario. With a total of 11 scenarios, 2750 Monte-Carlo simulations are performed.

### 3. Results & discussions

#### 3.1. Model calibration

The flow rate model for the sewer system includes both a conceptual model (for flow rate within the sub-catchments) and a detailed hydraulic model for the main sewer lines connecting the different sub-catchments and the WWTP. The modelled and measured flow rates at the WWTP inlet are in very good agreement (Fig. 5a). The model also captures the daily flow rate dynamics. The model simulates marginally higher peak flow rates during weekends as the underlying daily usage patterns are different for weekdays and weekends. The validation dataset also agrees very well with the model results (Fig. 5b). The higher peak flow rates in the weekend are noticed here as well. During the validation period, there are two instances where the measured flow rate is much higher than the modelled value. These are periods of wet weather flow. The model does not simulate the influence of rainfall/snowmelt etc. and hence cannot capture these trends. The datasets mainly include dry weather periods as the focus of the scenario analysis is on heat recovery during dry weather periods, which is the majority of the days during a year.

For the calibration period, while the temperature model can simulate the diurnal temperature dynamics for wastewater at WWTP influent reasonably well, the maximum and minimum daily temperature values are not always accurately predicted (Fig. 6a). The discrepancy between measured and modelled maximum and minimum daily temperature values is even higher in the validation period although the overall dynamics are captured by the model (Fig. 6b). One of the major reasons for the discrepancy in both the calibration and validation periods is due to lack of in-sewer air temperature measurements. Instead, ambient air temperature, which is easily available, is used in the model. It has earlier been observed the in-sewer air temperature has a higher correlation with sewer wastewater temperature than ambient air temperature (Saagi et al., 2021). Secondly, the difference in the model fit for calibration and validation is due to the more noisy ambient air temperature measurements during the validation period

leading to higher daily variations in wastewater temperature predictions (Fig. 6c, d). However, for both cases, model predictions are considered adequate as the goal of the modelling study is to perform scenario analysis and not an accurate prediction of the wastewater temperature at WWTP inlet. Secondly, comprehensive uncertainty analysis is employed to avoid relying on a single model calibration set for the scenario analysis.

#### 3.2. Scenario analysis

##### 3.2.1. Energy recovery potential for the different heat recovery locations

Heat recovery potential expectedly increases with increasing degree of implementation. During period 1, heat recovery at the shower (P1.I77) leads to maximum energy production (127 MWh/day for 180,000 domestic population equivalents) owing to its closeness to the wastewater generation source (showers), even though the heat recovery is through a heat exchanger (Fig. 7a, b). The household level heat recovery (P2.I77) gives the second best energy recovery (111 MWh/day) while the heat recovery at precinct levels (P3.I77) has an even lower energy recovery (92 MWh/day). The energy recovery values mentioned for the heat pumps are the net energy recovery after removing the energy input for heat pumps. During period 2, P1.I77 (96 MWh/day) and P3.I77 (96 MWh/day) have similar energy recovery followed by household heat recovery (P2.I77 – 77 MWh/day). It is interesting to note that heat recovery from P3.I77 was higher during period 2 (96 MWh/day) compared to period 1 (92 MWh/day) while it is the reverse for shower and household locations. This is due to the limitation in the design of the heat pumps that the internal coolant (cold media) cannot go below 0 °C. Since the incoming cold-water temperature is lower during period 1, this limitation is reached more frequently, leading to a drop in heat recovery potential. A different design where the internal coolant can be cooled to a lower temperature without the risk of freezing can extract even more energy during this period. For the shower and household locations, the heat recovery potential is higher during period 1 than period 2. This is due to the larger temperature difference between the incoming cold water and the outgoing wastewater. This is advantageous as the need for energy is also higher during the colder periods. Heat recovery from WWTP effluent results in a comparatively lower heat recovery potential (around 54 MWh/day for both the simulation periods) versus any of the other heat recovery scenarios with 77% degree of implementation. With 44% degree of implementation for any of the three locations, similar or higher energy than that recovered at the WWTP effluent is possible.

##### 3.2.2. WWTP influent temperature

The impact of the location of heat recovery on WWTP influent temperature is depicted in Fig. 8 for the different heat recovery positions (shower (P1), households (P2) and precinct (P3)) with varying degrees of implementation (16, 42, 77) using the calibrated model parameters (and without any uncertainty). The overall dynamics between 15 Jan. and 04 Feb. 2020

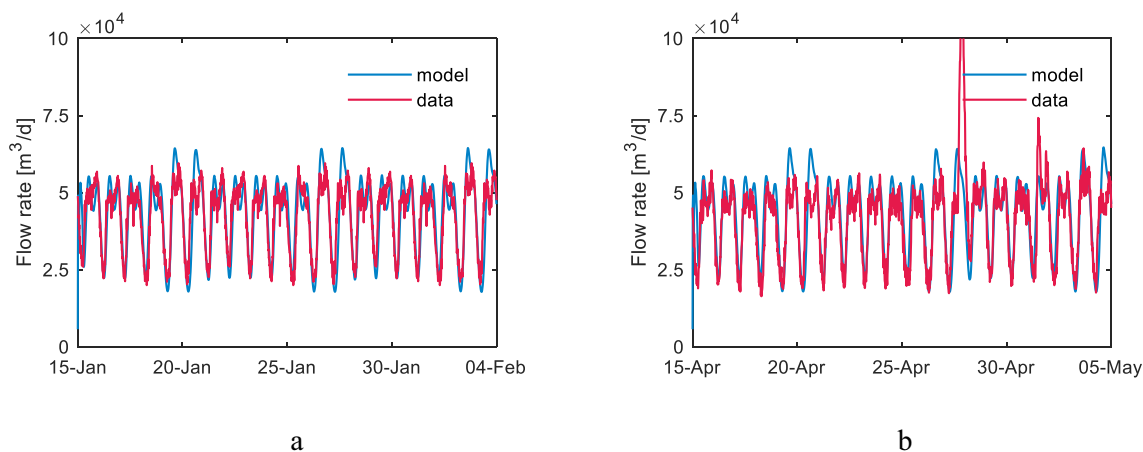
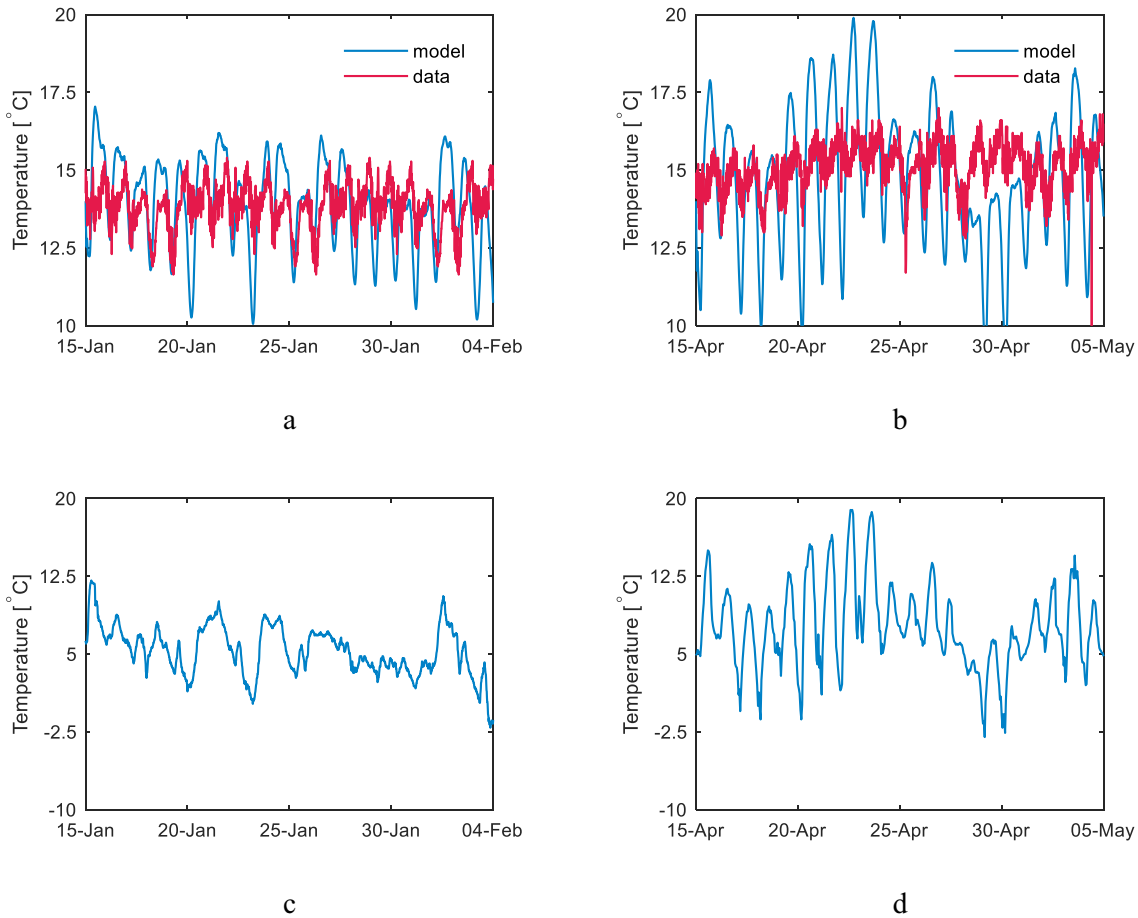


Fig. 5. Measured flow rate data at WWTP inlet compared with model results during calibration (a) and validation (b) periods.



**Fig. 6.** Modelled vs. measured wastewater temperature at the WWTP inlet for calibration (a) and validation (b) periods. Measured ambient air temperature for Linköping during calibration (c) and validation (d) periods.

(period 1) as well as a zoomed-in view of the trend on 20 Jan. 2020 is presented. The shower and household heat recovery scenarios show a similar and marginal impact on WWTP influent temperature (Fig. 8a, b, d, and e). The maximum reduction in WWTP influent temperature (compared to the default scenario) for shower and household heat recovery is 1.48 °C and 1.32 °C for scenarios P1.I77 and P2.I77, respectively. The daily variation in temperature for the heat exchangers at showers and households is very similar. The 16% implementation at both the locations does not show any noticeable difference in temperature dynamics at the WWTP inlet. A higher reduction in temperature is observed for the precinct level

heat recovery (P3.I77), where the mean WWTP inlet temperature difference between the default and P3.I77 scenario is 1.76 °C. A similar trend is noticed for the daily temperature dynamics with a more pronounced temperature variation (both in comparison to P1 and P2 as well as for the different degrees of implementation at P3). This is because the precinct level heat pumps are located comparatively closer to the WWTP versus the heat exchangers at showers and households (Fig. 8c, f). A substantial drop in temperature already happens (even without any heat recovery) before the wastewater reaches the precinct heat recovery location, further heat recovery using heat pumps leads to a lower WWTP inlet temperature

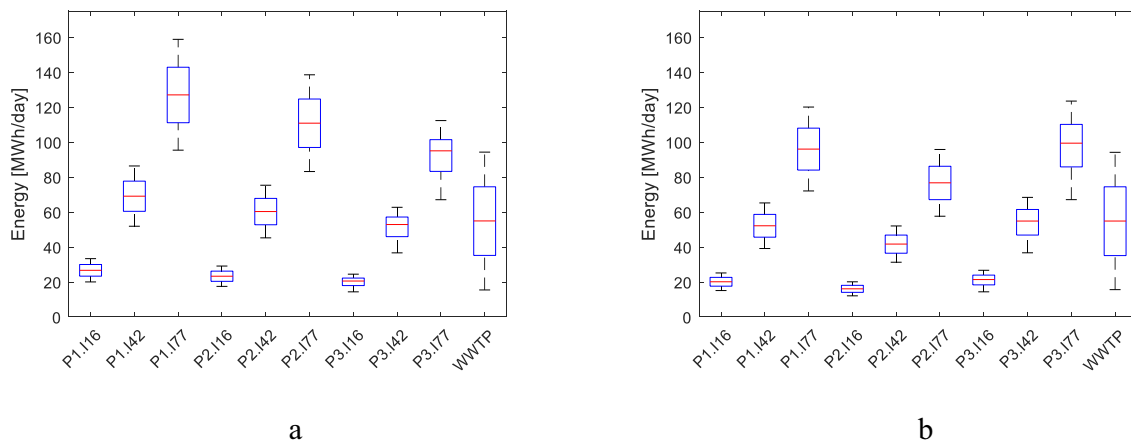


**Fig. 7.** Variation in energy recovery for the different heat recovery scenarios with uncertainty during calibration (a) and validation (b) periods.



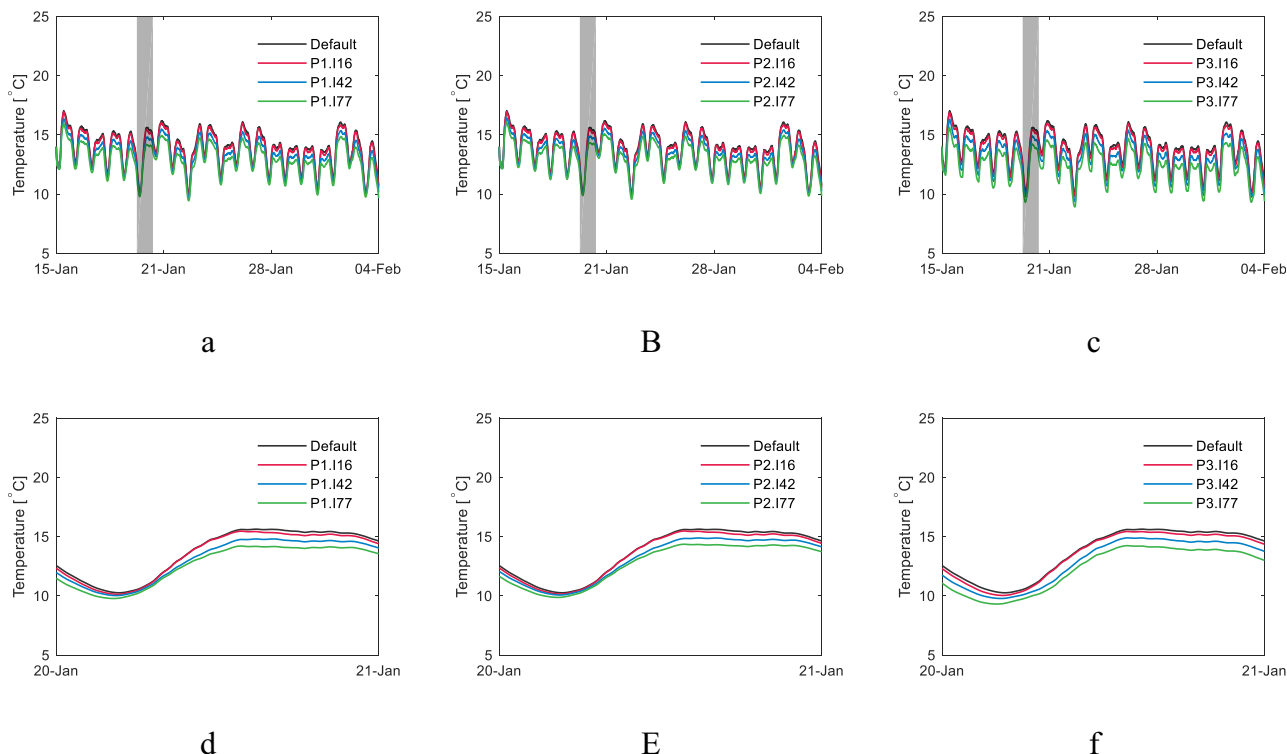


Fig. 8. Overview of modelled WWTP inlet temperature for showers (a), households (b) and precincts (c) with varying levels of heat recovery (16, 42, 77) during the period 15 Jan. to 04 Feb. Zoomed-in model predictions on 20th Jan. 2020 for showers (d), households (e) and precincts (f).

compared to other scenarios (P1 and P2). Secondly, heat exchangers are used at showers and households while heat pumps are used at precinct level allowing for a more efficient heat recovery resulting in a higher wastewater temperature reduction. For the scenarios with 16% heat recovery, the maximum reduction in temperature noticed is 0.31 °C, 0.27 °C and 0.34 °C for showers, household and precincts. Similarly, 0.89 °C, 0.77 °C and 1.11 °C temperature reduction is observed for scenarios P1.I42, P2.I42 and P3.I42, respectively. Overall, even for the highest degree of implementation (77% of domestic flow rate), the maximum drop in the wastewater temperature at WWTP inlet is less than 2 °C.

Based on the uncertainty analysis, the mean influent wastewater temperature without any heat recovery during the evaluation period is 13.97 °C and 15.21 °C for 15 Jan.–04 Feb. 2020 (period 1) and 15 April–04 May 2020 (period 2), respectively. The effect on WWTP influent temperature is negligible (less than 0.25 °C reduction in temperature compared to the

default scenario) for the 16% heat recovery at all locations (Fig. 9a, b). The mean temperature difference between the default scenarios and any of the shower and household heat recovery scenarios is always less than or equal to 1 °C. The precinct 77% leads to the highest reduction in mean wastewater temperatures for both the periods (1.43 °C and 1.50 °C for period 1 and period 2, respectively). The drop in average temperature can be considered as low for such a high degree of implementation. The WWTP effluent heat recovery does obviously not have any impact on WWTP inlet temperature. By analyzing the heat recovery potential results together with the WWTP inlet temperature results, the highest heat recovery potential (127 MWh/day) together with an almost negligible impact on wastewater temperature at WWTP inlet is for the shower heat recovery (P1.I77) during period 1. The results indicate that heat recovery from locations that are farthest from the WWTP (showers, households) have the least impact on WWTP inlet temperature. A similar and encouraging trend is also

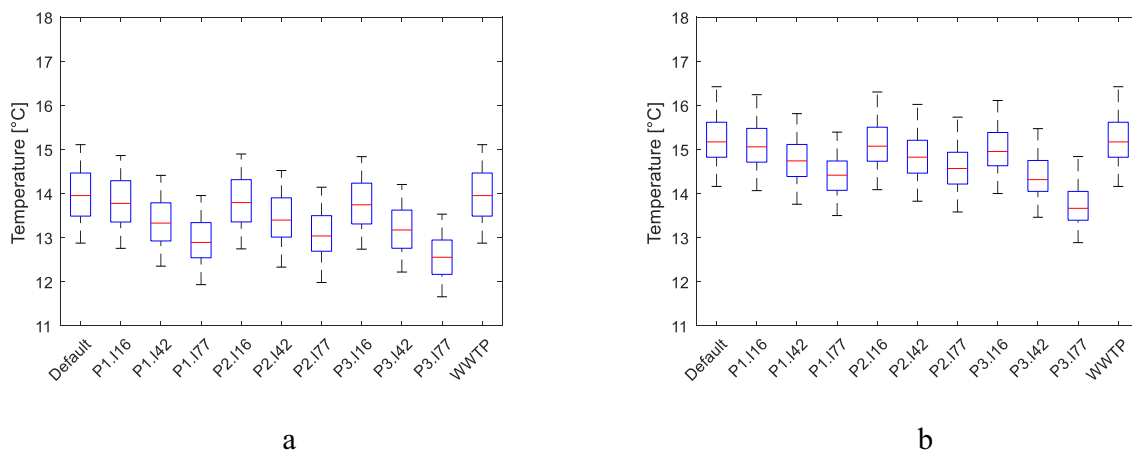


Fig. 9. Box plots depicting the mean inlet WWTP temperature for the different scenarios with uncertainty for both calibration (a) and validation (b) periods.

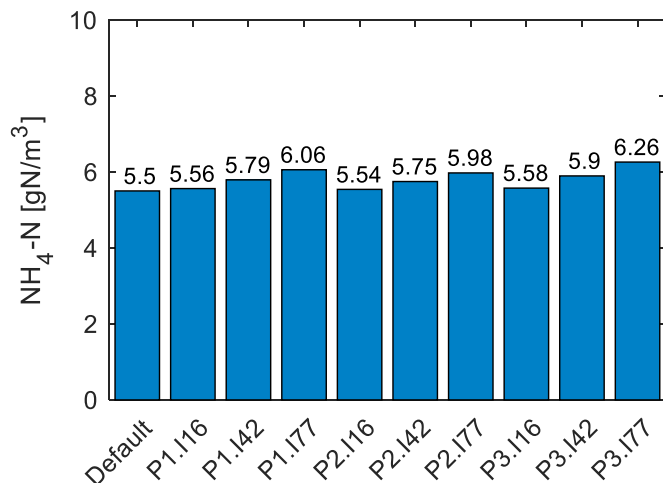


Fig. 10. Variation in NH<sub>4</sub>-N concentration at the secondary clarifier effluent for the different heat recovery scenarios during period 1.

clearly observed in various other studies on heat recovery from wastewater (Hadengue et al., 2021). Due to the long sewer network between the farthest locations and WWTP, thermal damping (heat loss to the surroundings) in the sewers will result in losing most of this heat content even in the absence of heat recovery equipment. The closer the location of heat recovery equipment to the WWTP, the higher is the difference in WWTP inlet temperature with and without heat recovery. This is because of the limited thermal damping due to the shorter distance from the WWTP inlet.

### 3.2.3. WWTP performance – impact on NH<sub>4</sub>-N removal

With lower temperatures, the NH<sub>4</sub>-N concentration in the secondary clarifier effluent increases with decreasing temperature indicating reduced nitrification capacity (Fig. 10). The NH<sub>4</sub>-N concentration with 16% degree of implementation for showers, households and precincts is 5.56 gN/m<sup>3</sup>, 5.54 gN/m<sup>3</sup> and 5.58 gN/m<sup>3</sup>, respectively. These values are very similar to the NH<sub>4</sub>-N concentration at the secondary clarifier effluent for the default scenario (5.5 gN/m<sup>3</sup>). The highest NH<sub>4</sub>-N concentration is noticed for 77% implementation for precincts (6.26 gN/m<sup>3</sup>), followed by showers (6.06 gN/m<sup>3</sup>) and households (5.98 gN/m<sup>3</sup>). The trend observed for the NH<sub>4</sub>-N concentration increase matches with that observed for reduction in WWTP inlet temperature (Fig. 9). This is expected and agrees with other studies regarding the impact of wastewater temperature on nitrification (Wanner et al., 2005). The increase is however only minimal due case specific factors: i) the intermittent aeration is controlled towards an ammonia threshold leading to extended aeration time when temperature is

decreased; and ii) the relatively high wastewater temperature in the default case for both periods.

However, the WWTP effluent NH<sub>4</sub>-N concentration is reduced, although only marginally with decreasing temperature (Fig. 11 a, b). During period 1, for the scenarios with maximum heat recovery at the three locations (P1.I77, P2.I77 and P3.I77), the mean effluent NH<sub>4</sub>-N concentration is 0.70 gN/m<sup>3</sup>, 0.70 gN/m<sup>3</sup> and 0.68 gN/m<sup>3</sup>, respectively, in comparison to the default scenario with 0.75 gN/m<sup>3</sup>. A similar trend is also observed during period 2, where the mean effluent NH<sub>4</sub>-N concentration reduced by a maximum of 0.2 gN/m<sup>3</sup>. Also, the lowest mean effluent NH<sub>4</sub>-N concentration in period 1 is 0.68 gN/m<sup>3</sup> compared to 0.76 gN/m<sup>3</sup> during period 2 even though WWTP inlet temperature is lower in the first period.

Simulations from period 1 with the default calibration parameters are used to analyze this counter-intuitive observation further. While the NH<sub>4</sub>-N concentration in the secondary clarifier effluent increases with decreasing temperature, the effluent NO<sub>x</sub>-N concentration in the secondary clarifier effluent also increases (Fig. 12a). This is due to the intermittent aeration control in the activated sludge reactors. This control increases the aeration time during low temperatures to improve nitrification (Fig. 12b). The aeration time increases marginally with increasing heat recovery percentage for the three locations. This results in a reduction in the denitrification capacity and hence a higher NO<sub>x</sub>-N concentration is seen in the activated sludge effluent. The subsequent ozonation step leads to a very high DO concentration in the wastewater that goes to the post N-DN reactors. In the post N-DN process using an MBBR, the NO<sub>x</sub>-N control strategy reduces the excess nitrate by increasing the carbon dosing. The increased carbon dosing combined with the high oxygen availability and the resulting higher heterotrophic biomass concentration leads to a higher consumption of NH<sub>4</sub>-N as the nitrogen source for growth. This series of events – a higher nitrate concentration in the activated sludge effluent due to intermittent aeration control; a higher heterotrophic biomass concentration due to carbon dosing and high dissolved oxygen availability leading to more NH<sub>4</sub>-N consumption are causing the lowering of NH<sub>4</sub>-N concentration with lowering temperatures.

In summary, it should be noted that the marginal decrease in the simulated effluent NH<sub>4</sub>-N with lower WWTP inlet temperature is only specific to this WWTP. In fact, the differences are minimal and for practical purposes and given the uncertainty range, the effluent NH<sub>4</sub>-N concentration is not impacted for the simulated heat recovery scenarios.

### 3.3. Future research

Several potential measures to improve model prediction accuracy are: 1. The use of in-sewer air temperature instead of ambient air temperature for the sewer model; 2. Soil temperature measurements at different locations in the city at the sewer depth levels; 3. Sewer wastewater temperature

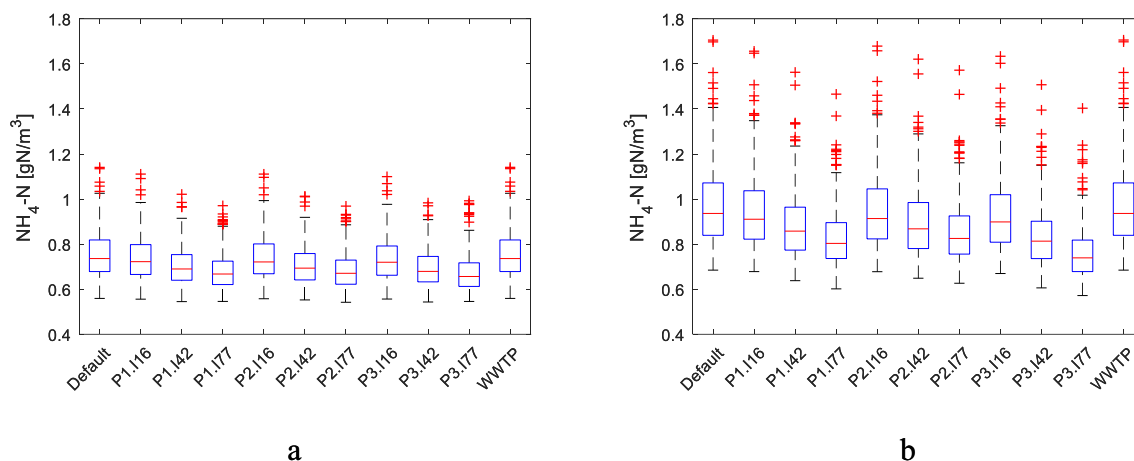


Fig. 11. Linköping WWTP effluent NH<sub>4</sub>-N concentration for the different heat recovery scenarios with uncertainty during the calibration (a) and validation (b) periods.

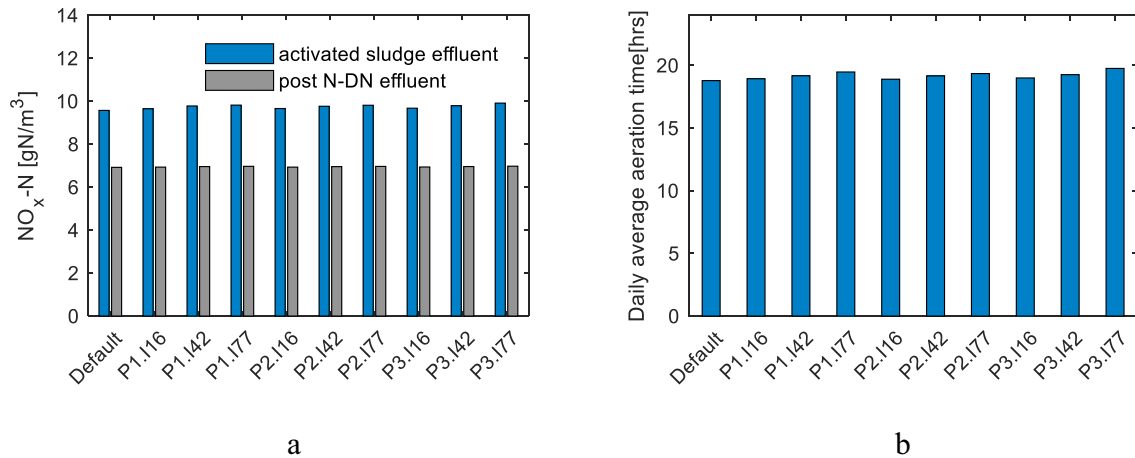


Fig. 12. NO<sub>x</sub>-N (a) concentrations in the activated sludge reactor and post N-DN reactor effluents and the daily aeration time for the reactor (b) for different heat recovery scenarios during calibration period without uncertainty.

data at different sewer locations in the city (Abdel-Aal et al., 2018) to facilitate model performance evaluation at multiple points; and, 4. Dry weather infiltration (from groundwater sources) flow rate and temperature data. Additionally, the design of heat pumps used in this model is scaled based on one potential design example from a heat pump supplier. However, it was clear that the design is case-specific and can vary depending on the location and heat utilization options. The availability of more information on heat pump design can be further used to reduce the uncertainty used for the heat pump model parameters.

Aspects that are not currently included but can be of interest for future development are: i. The impact of temperature on sewer biological and physico-chemical characteristics (e.g. grease and oil deposits, hydrogen sulphide production etc.). ii. Impact of wastewater temperature on separation processes in the WWTP. The primary and secondary clarifier models currently used do not consider any temperature impacts on settling efficiency; and, iii. Long-term impact on maximum plant load and life span even if the current performance is not reduced significantly with heat recovery.

To arrive at a holistic decision-making regarding heat recovery from wastewater, several other socio-economic aspects should be considered while this study solely focused on the technical aspects. Life cycle analysis, life cycle costs and cost-benefit analysis for the different implementations have not been performed. It should be noted that a large number of installations at each building are needed for shower and household level heat recovery while the precinct level heat recovery requires much fewer and larger heat pumps installed. Another aspect to consider in the decision-making is – who profits from the recovered heat? For shower and households, it is the individual apartment/housing association owners while at the precinct and WWTP level heat recovery is mainly used by municipalities in Sweden.

#### 4. Conclusions

A model-based study integrating the different sub-models (wastewater generation, heat transfer in the sewer network, heat recovery equipment, wastewater treatment) is applied to evaluate heat recovery potential at several locations for a Swedish city (Linköping) using an uncertainty-based approach. Key conclusions are:

- Heat recovery at showers (P1.I77) leads to the highest mean energy recovery (127 MWh/day) while the mean wastewater temperature drop compared to the default (no heat recovery) scenario at WWTP inlet is less than 0.25 °C.
- Maximum drop in mean wastewater temperature at WWTP inlet is 1.5 °C for the scenario with heat recovery at precincts (P3.I77) during evaluation period 2.
- The impact on nitrification at the WWTP is minimal partly owing to the

special configuration of the WWTP.

- Energy recovery potential varies across the year with higher recovery potential during colder periods. This is due to a larger temperature difference between the incoming cold water and the wastewater.
- The farther the location of heat recovery equipment from the WWTP, the lower is the impact on wastewater temperature at the WWTP inlet.
- Heat recovery from wastewater at any of the potential locations is still favorable with limited impact on WWTP performance for the specific case-study.

#### CRediT authorship contribution statement

**Ramesh Saagi:** Conceptualization, Methodology, Software, Formal Analysis, Writing – Original Draft, Visualization. **Magnus Arnell:** Conceptualization, Methodology, Software, Writing – Review & Editing, Supervision, Project administration, Funding acquisition. **Christoffer Wärff:** Conceptualization, Methodology, Software, Formal Analysis, Writing – Review & Editing. **Marcus Ahlström:** Conceptualization, Methodology, Software, Formal Analysis, Writing – Review & Editing. **Ulf Jeppsson:** Conceptualization, Methodology, Formal Analysis, Supervision, Project administration, Funding acquisition.

#### Declaration of competing interest

The authors declare that they have no known competing financial interests or personal relationships that could have appeared to influence the work reported in this paper.

#### Acknowledgements

The authors acknowledge the financial support provided by the Swedish research council Formas (942-2016-80), Swedish Water (16-106), Sweden Water Research, and Tekniska Verken i Linköping for the project HÅVA (“Sustainability analysis for heat recovery from wastewater”). Tekniska Verken i Linköping is also gratefully acknowledged for their financial support and for supporting measurement campaigns. The computations were performed on resources provided by the Swedish National Infrastructure for Computing (SNIC) through the Center for Scientific and Technical Computing at Lund University (LUNARC) under project LU 2020/2-32.

#### References

- Abdel-Aal, M., Smits, R., Mohamed, M., De Gussem, K., Schellart, A., Tait, S., 2014. Modelling the viability of heat recovery from combined sewers. *Water Sci. Technol.* 70 (2), 297–306. <https://doi.org/10.2166/wst.2014.218>.

- Abdel-Aal, M., Schellart, A., Kroll, S., Mohamed, M., Tait, S., 2018. Modelling the potential for multi-location in-sewer heat recovery at a city scale under different seasonal scenarios. *Water Res.* 145, 618–630. <https://doi.org/10.1016/j.watres.2018.08.073>.
- Arnell, M., Saagi, R., 2020. Modelling of heat recovery equipment. Technical Report No. CODEN:LUTEDX/(TEIE-7280)/1-8/(2020). Division of Industrial Electrical Engineering and Automation, Lund University, Sweden.
- Arnell, M., Lundin, E., Jeppsson, U., 2017. Sustainability analysis for wastewater heat recovery – literature review. Technical Report No. LUTEDX/(TEIE-7267)/1-41/(2017). Division of Industrial Electrical Engineering and Automation, Lund University, Sweden.
- Arnell, M., Ahlström, M., Wärrf, C., Saagi, R., Jeppsson, U., 2021. Plant-wide modelling and analysis of WWTP temperature dynamics for sustainable heat recovery from wastewater. *Water Sci. Technol.* 84 (4), 1023–1036. <https://doi.org/10.2166/wst.2021.277>.
- Chae, K.-J., Ren, X., 2016. Flexible and stable heat energy recovery from municipal wastewater treatment plants using a fixed-inverter hybrid heat pump system. *Appl. Energy* 179, 565–574. <https://doi.org/10.1016/j.apenergy.2016.07.021>.
- Directive (EU) 2018/2001, 2018. Directive (EU) 2018/2001 of the European Parliament and of the Council - of 11 December 2018 - On the Promotion of the Use of Energy From Renewable Sources. L328, pp. 82–209.
- Dürrenmatt, D.J., Wanner, O., 2014. A mathematical model to predict the effect of heat recovery on the wastewater temperature in sewers. *Water Res.* 48, 548–558. <https://doi.org/10.1016/j.watres.2013.10.017>.
- Elías-Maxil, J.A., Hofman, J., Wols, B., Clemens, F., van der Hoek, J.P., Rietveld, L., 2017. Development and performance of a parsimonious model to estimate temperature in sewer networks. *Urban Water J.* 14 (8), 829–838. <https://doi.org/10.1080/1573062X.2016.1276811>.
- European Union, 2019. EU Energy in Figures – Statistical Pocket Book. Publications Office of the European Union, Luxembourg.
- Fernández-Arévalo, T., Lizarralde, I., Grau, P., Ayesa, E., 2014. New systematic methodology for incorporating dynamic heat transfer modelling in multi-phase biochemical reactors. *Water Res.* 60, 141–155. <https://doi.org/10.1016/j.watres.2014.04.034>.
- Fernández-Arévalo, T., Lizarralde, I., Fdz-Polanco, F., Pérez-Elvira, S.I., Garrido, J.M., Puig, S., Poch, M., Grau, P., Ayesa, E., 2017. Quantitative assessment of energy and resource recovery in wastewater treatment plants based on plant-wide simulations. *Water Res.* 118, 272–288. <https://doi.org/10.1016/j.watres.2017.04.001>.
- Figuerola, A., Hadengue, B., Leitão, J.P., Rieckermann, J., Blumensaat, F., 2021. A distributed heat transfer model for thermal-hydraulic analyses in sewer networks. *Water Res.* 204, 117649. <https://doi.org/10.1016/j.watres.2021.117649>.
- Forsberg, L.S., Torstensson, G., Johansson, G., 2012. Växtnäringsförluster i små jordbruksdominerade avrinningsområden 2010/2011 (Plant nutrient losses in small agriculture dominant catchment areas 2010/2011). Swedish University of Soil and Environment, Uppsala, Sweden (in Swedish).
- Gatto, A., Drago, C., 2020. Measuring and modeling energy resilience. *Ecol. Econ.* 172, 106527. <https://doi.org/10.1016/j.ecolecon.2019.106527>.
- Geankoplis, C.J., 1993. Transport Processes and Unit Operations. 3rd ed. Pearson College Division, New York, USA.
- Benchmarking of control strategies for wastewater treatment plants. In: Gernaey, K.V., Jeppsson, U., Vanrolleghem, P.A., Copp, J.B. (Eds.), Scientific and Technical Report No. 23. IWA Publishing <https://doi.org/10.2166/9781780401171>.
- Golzar, F., Silveira, S., 2021. Impact of wastewater heat recovery in buildings on the performance of centralized energy recovery – a case study of Stockholm. *Appl. Energy* 297, 117141. <https://doi.org/10.1016/j.apenergy.2021.117141>.
- Hadengue, B., Joshi, P., Figuerola, A., Larsen, T.A., Blumensaat, F., 2021. In-building heat recovery mitigates adverse temperature effects on biological wastewater treatment: a network-scale analysis of thermal-hydraulics in sewers. *Water Res.* 204, 117552. <https://doi.org/10.1016/j.watres.2021.117552>.
- Hadengue, B., Morgenroth, E., Larsen, T.A., Baldini, L., 2022. Performance and dynamics of active greywater heat recovery in buildings. *Appl. Energy* 305, 117677. <https://doi.org/10.1016/j.apenergy.2021.117677>.
- Henze, M., Gujer, W., Mino, T., van Loosdrecht, M., 2000. Activated sludge models ASM1, ASM2, ASM2d and ASM3. Scientific and Technical Report No. 9. IWA Publishing, London, UK.
- Iman, R.L., Conover, W.J., 1982. A distribution-free approach to inducing rank correlation among input variables. *Commun. Stat. Simul. Comput.* 11 (3), 311–334. <https://doi.org/10.1080/03610918208812265>.
- Kjellander, K., 2015. Two simple soil temperature models: applied and tested on sites in Sweden. Technical Report. Uppsala University, Uppsala, Sweden.
- Larsen, T.A., 2015. CO<sub>2</sub>-neutral wastewater treatment plants or robust, climate-friendly wastewater management? A systems perspective. *Water Res.* 87, 513–521. <https://doi.org/10.1016/j.watres.2015.06.006>.
- Lippi, S., Rosso, D., Lubello, C., Canziani, R., Stenstrom, M.K., 2009. Temperature modelling and prediction for activated sludge systems. *Water Sci. Technol.* 59 (1), 125–131. <https://doi.org/10.2166/wst.2009.587>.
- Makinia, J., Wells, S.A., Zima, P., 2005. Temperature modeling in activated sludge systems: a case study. *Water Environ. Res.* 77 (5), 525–532. <https://doi.org/10.2175/106143005X67449>.
- Nagpal, H., Spriet, J., Murali, M.K., McNabola, A., 2021. Heat recovery from wastewater – a review of available resource. *Water* 13 (9), 1274. <https://doi.org/10.3390/w13091274>.
- Olsson, G., 2012. ICA and me – a subjective review. *Water Res.* 46 (6), 1585–1624. <https://doi.org/10.1016/j.watres.2011.12.054>.
- Petersen, A.B., 2018. ReUseHeat Handbook – Experiences From Other Urban Waste Heat Recovery Investments. Grøn Energi (DDHA), Kolding, Denmark.
- Rieger, L., Gillot, S., Langergraber, G., Ohtsuki, T., Shaw, A., Takács, I., Winkler, S., 2012. Guidelines for using activated sludge models. Scientific and Technical Report No. 22. IWA Publishing, London, UK.
- Saagi, R., Arnell, M., Reyes, D., Wärrf, C., Ahlström, M., Jeppsson, U., 2021. Modelling temperature dynamics in sewer systems – comparing mechanistic and conceptual modelling approaches. *Water Sci. Technol.* <https://doi.org/10.2166/wst.2021.425> Online.
- Saltelli, A., Ratto, M., Andres, T., Campolongo, F., Cariboni, J., Gatelli, D., Saisana, M., Tarantola, S., 2008. Global Sensitivity Analysis: The Primer. John Wiley & Sons, Hoboken, NJ, USA.
- Šimůnek, J., Genuchten, M.Th., Šejna, M., 2016. Recent developments and applications of the HYDRUS computer software packages. *Vadose Zone J.* 15 (7), 1–25. <https://doi.org/10.2136/vzj2016.04.0033>.
- Sin, G., Gernaey, K.V., Neumann, M.B., van Loosdrecht, M.C.M., Gujer, W., 2009. Uncertainty analysis in WWTP model applications: a critical discussion using an example from design. *Water Res.* 43 (11), 2894–2906. <https://doi.org/10.1016/j.watres.2009.03.048>.
- Sitzenfrei, R., Hillebrand, S., Rauch, W., 2017. Investigating the interactions of decentralized and centralized wastewater heat recovery systems. *Water Sci. Technol.* 75 (5), 1243–1250. <https://doi.org/10.2166/wst.2016.598>.
- Spriet, J., McNabola, A., Neugebauer, G., Stoeglehner, G., Ertl, T., Kretschmer, F., 2020. Spatial and temporal considerations in the performance of wastewater heat recovery systems. *J. Clean. Prod.* 247, 119583. <https://doi.org/10.1016/j.jclepro.2019.119583>.
- The Swedish Energy Agency, 2009. Mätning av kall- och varmvattenanvändning i 44 hushåll (Measurement of cold and hot water usage in 44 households). Technical Report No. ER 2009:26. Swedish Energy Agency, Eskilstuna, Sweden.
- Tikhonova, A., 2018. Värmebalans av Käppalaverket och optimering av värmeflöden (Heat balance of Käppalaverket and optimization of heat flows). MSc thesis Uppsala University, Uppsala, Sweden (in Swedish).
- Vavříčka, R., Boháč, J., Matuška, T., 2022. Experimental development of the plate shower heat exchanger to reduce the domestic hot water energy demand. *Energy Build.* 254, 111536. <https://doi.org/10.1016/j.enbuild.2021.111536>.
- Wallin, J., 2021. Case studies of four installed wastewater heat recovery systems in Sweden. *Case Stud. Therm. Eng.* 26, 101108. <https://doi.org/10.1016/j.csite.2021.101108>.
- Wanner, O., Panagiotidis, V., Clavadetscher, P., Siegrist, H., 2005. Effect of heat recovery from raw wastewater on nitrification and nitrogen removal in activated sludge plants. *Water Res.* 39 (19), 4725–4734. <https://doi.org/10.1016/j.watres.2005.09.026>.
- Wärrf, C., Arnell, M., Sehlén, R., Jeppsson, U., 2020. Modelling heat recovery potential from household wastewater. *Water Sci. Technol.* 81 (8), 1597–1605. <https://doi.org/10.2166/wst.2020.103>.